Inorganica Chimica Acta 444 (2016) 159–165

Contents lists available at ScienceDirect

Inorganica Chimica Acta

journal homepage: www.elsevier.com/locate/ica

A dinuclear iron(II) complex bearing multidentate pyridinyl ligand: Synthesis, characterization and its catalysis on the hydroxylation of aromatic compounds

Erxing Gu [a], Wei Zhong [b,*], Hongxia Ma [b], Beibei Xu [c], Hailong Wang [b], Xiaoming Liu [b,*]

[a] School of Metallurgy and Chemical Engineering, Jiangxi University of Science and Technology, Ganzhou 341000, China
[b] College of Biological, Chemical Sciences and Engineering, Jiaxing University, Jiaxing 314001, China
[c] School of Chemistry, Nanchang University, Nanchang 330031, China

ARTICLE INFO

Article history:
Received 2 December 2015
Received in revised form 31 January 2016
Accepted 2 February 2016
Available online 6 February 2016

Keywords:
Diiron complex
Hydroxylation
Aromatic compounds
Catalysis
Phenols

ABSTRACT

A dinuclear iron(II) complex $Fe_2\mathbf{L}_2(\mu_2\text{-}Cl)_2Cl_2$ (**L** = N,N-bis(pyridin-2-ylmethyl)prop-2-yn-1-amine) was prepared and fully characterized by UV–Vis spectroscopy, elemental analysis, electrochemical analysis and X-ray single crystal diffraction analysis. The catalytic activity of the complex was assessed for the hydroxylation of aromatic compounds by using aqueous H_2O_2 as an oxidant in acetonitrile. The catalytic system was applicable in a wide range of substrates including aromatic compounds with both electron-donating and electron-withdrawing substituents and showed moderate to good catalytic activity and selectivity in the oxidation reactions. Particularly, in the case of benzene the selectivity of phenol achieve to 74% with the reaction conversion of 24.8%.

1. Introduction

A variety of iron complexes have been widely used as homogenous catalysts for the preparation of important organic molecules, including commodity chemicals, pharmaceuticals and polymers [1–5]. The enthusiasm in the research of iron-based catalysts has been due to not only that iron is inexpensive, earth-abundant and non-toxic, but also that in many enzymes, iron-based enzymes catalyze some important reactions under physiological conditions, such as the activation of O_2 and C—H bonds [6–9]. Largely due to the biological inspiration, various dinuclear iron complexes were synthesized to mimic such diiron enzyme and their catalytic properties were well studied. [FeFe]-hydrogenase [10–13] and soluble methane monooxygenase [14] are such an example. The former catalyzes both evolution and oxidation of hydrogen at remarkable efficiency and rate and the latter catalyzes the hydroxylation of methane into methanol [15,16]. In general, the coordination chemistry of the iron centers in those iron enzymes is well satisfied by the ligands (usually amino acid residues of proteins) of N, O, S ligating atoms, which alongside with the proximal environment offered by protein domains render the enzymes specific functionalities. Thus, the search for new catalytic systems based on iron complexes with nitrogen ligands has been the subject of extensive studies, with the final aim to mimic the catalytic properties of natural enzymes.

Inspired by some base metals complexes such as iron [17–20] and copper [21–24] (either mono- or multi-nuclear) exhibiting functionalities of catalysis on hydroxylation of aromatic compounds, we have been interested in exploring the catalytic chemistry of iron and copper complexes bearing multidentate ligand containing N, O atoms by tuning their electronic and structural properties. Recently, we have reported such catalytic systems basing on iron [25] and copper complexes [26,27] for the hydroxylation of benzene. The results showed that the catalytic efficiency of the complexes correlates well with their reduction potentials, that is, the more negative the reduction potential of these complexes, the higher the benzene conversion. Even though the conversion of benzene achieves over 40%, the selectivity of phenol is less than 50%. Thus, how to avoid the over-oxidation of phenol to improve the selectivity/yield becomes a huge challenge in the homogeneous catalytic hydroxylation of benzene.

In this piece of work, we report the fully characterization of a dinuclear iron(II) complex $Fe_2\mathbf{L}_2(\mu_2\text{-}Cl)_2Cl_2$ (**L** = N,N-bis(pyridin-2-ylmethyl)prop-2-yn-1-amine) containing multidentate pyridinyl ligand and its catalysis on the hydroxylation of a variety of aromatic compounds including benzene under mild conditions

---

* Corresponding authors. Tel./fax: +86 (0)573 83643937.
E-mail addresses: weizhong@mail.zjxu.edu.cn (W. Zhong), xiaoming.liu@mail.zjxu.edu.cn (X. Liu).

http://dx.doi.org/10.1016/j.ica.2016.02.005
0020-1693/

(at 70 °C in acetonitrile solution) with hydrogen peroxide. Although the influence was not significant, our results did show that the electronic property of the substituent group(s) on an aromatic compound exerted influence on both conversion and selectivity.

2. Experimental

2.1. General procedures

Unless otherwise stated, all chemicals and solvents were of AR grade and purchased from local suppliers unless otherwise stated. The organic solvents used in this work were appropriately dried when necessary. Elemental analyses were performed on a CHN elemental analyzer and used Elementar Vario MICRO. UV–Vis spectra were recorded in the range of 200–800 nm on a VARIAN 50 Conc in acetonitrile. Electrochemistry was performed in a gas-tighten three-electrode system in which a vitreous carbon disk ($\Phi = 1$ mm) was used as a working electrode, a carbon strip as counter electrode, and Ag/AgCl (inner reference solution: 0.45 mol L^{-1} [N^{n}Bu$_4$]BF$_4$ + 0.05 mol L^{-1} [N^{n}Bu$_4$]Cl in dichloromethane) against which the potential of ferrocenium/ferrocene couple is 0.55 V in 0.5 mol L^{-1} [N^{n}Bu$_4$]BF$_4$ in dichloromethane as described elsewhere [28,29]. Ferrocene was added as an internal standard and all potentials are quoted against ferrocenium/ferrocene couple (Fc$^+$/Fc). Crystallographic data of complex $Fe_2\mathbf{L}_2(\mu_2\text{-}Cl)_2Cl_2$ were collected on a Bruker SMART CCD diffractometer with graphite-monochromated Mo Kα radiation ($\lambda = 0.71073$ Å). The crystal structures were solved using direct methods in SHELXS and refined by full-matrix least-squares routines, based on F^2, using the SHELXL package [30].

2.2. Synthesis of iron(II) complex $Fe_2\mathbf{L}_2(\mu\text{-}Cl)_2Cl_2$

The ligand **L** (474 mg, 2 mmol) was dissolved in degassed methanol (10 mL) and then the degassed methanolic solution of $FeCl_2{\cdot}4H_2O$ (397 mg, 2 mmol) was added into the above solution. The mixture was stirred for 3 h under argon atmosphere at room temperature to afford yellow solid. The solution was removed under reduced pressure to collect the yellow solid (550 mg, 76%), which was washed with water (3 × 30 mL) and diethyl ether (3 × 30 mL) successively, and then dried in vacuo. Dark yellow crystals suitable for X-ray analysis were obtained from its solution in a mixture of diethyl ether–methanol in a few days at room temperature. Elemental analysis calculated for $C_{30}H_{30}N_6Fe_2Cl_4$: Calc. C, 49.49; H, 4.15; N, 11.54; found: C, 49.46; H, 4.10; N, 11.18%.

2.3. Catalytic assessment

A typical procedure is as follows: Benzene (0.9 mL, 10 mmol), acetonitrile (3.8 mL) and catalytic amount of the iron(II) complex (2‰) were placed into the reaction vessel (10 mL), which is equipped with cooling condenser and placed in an oil-bath. The reaction was heated and when the temperature reached 70 °C, aqueous H_2O_2 (30 wt%, 1.2 mL, 12 mmol) was slowly and carefully added in one-go. After heated at 70 °C for 2 h, the reaction was stopped and the volume of the mixture was calibrated to 10 mL with CH_3CN. To the calibrated reaction solution was added $MgSO_4$ (3.0 g) to remove the water in the reaction before being analyzed by gas chromatography (GC 7820A) with a packed column of Restek capillary SE-54 and using toluene as an internal standard. The temperature of the GC column was set at 60 °C for 1 min and then was programed to rise to 160 °C at the rate of 10 °C min^{-1}. Under the employed conditions, the retention time for benzene, toluene, benzoquinone and phenol were 3.3 ± 0.2 min,

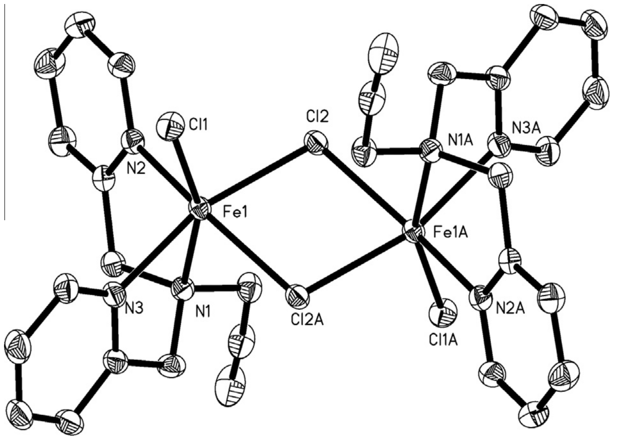

Fig. 1. Crystal structure of complex $Fe_2\mathbf{L}_2(\mu_2\text{-}Cl)_2Cl_2$.

Table 1
Crystallographic details and refinement data for complex $Fe_2\mathbf{L}_2(\mu_2\text{-}Cl)_2Cl_2$.

Empirical formula	$C_{30}H_{30}Cl_4N_6Fe_2$
F_w	728.10
Crystal system	monoclinic
Space group	*P*2(1)/*c*
Unit cell dimensions	
a (Å)	10.0015(7)
b (Å)	17.0150(12)
c (Å)	10.0015(7)
α (°)	90
β (°)	110.01
γ (°)	90
V (Å^3)	1599.25(19)
Z	2
D_{calc} (Mg m^3)	1.512
F(000)	744
Reflections collected (R_{int})	14765 (0.0223)
Reflections independent	3936
Goodness-of-fit on F^2	1.024
R_1, wR_2 [$I > 2\sigma(I)$]	0.0235, 0.0643
R_1, wR_2 (all data)	0.0261, 0.0662

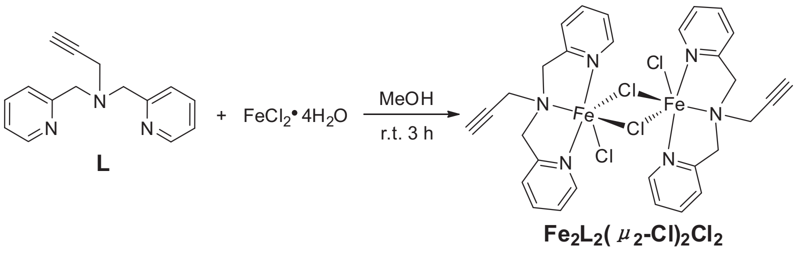

Scheme 1. Synthesis of dinuclear iron(II) complex $Fe_2\mathbf{L}_2(\mu_2\text{-}Cl)_2Cl_2$.

Table 2
Selected bond distances (Å) and angles (°) for complex $Fe_2\mathbf{L}_2(\mu_2\text{-}Cl)_2Cl_2$.

Fe(1)—N(1)	2.3126(11)	Fe(1)—Cl(1)	2.3667(4)
Fe(1)—N(2)	2.2083(11)	Fe(1)—Cl(2)	2.4797(4)
Fe(1)—N(3)	2.2156(11)	Fe(1)—Cl(2A)	2.5445(4)
Fe(1)…Fe(1A)	3.803(4)		
N(1)—Fe(1)—N(2)	74.80(4)	N(3)—Fe(1)—Cl(2)	164.46(3)
N(2)—Fe(1)—N(3)	99.64(4)	N(1)—Fe(1)—Cl(2A)	92.42(3)
N(1)—Fe(1)—N(3)	72.55(4)	N(2)—Fe(1)—Cl(2A)	163.22(3)
N(1)—Fe(1)—Cl(1)	159.81(3)	N(3)—Fe(1)—Cl(2A)	86.46(3)
N(2)—Fe(1)—Cl(1)	93.78(3)	Cl(1)—Fe(1)—Cl(2A)	101.470(14)
N(3)—Fe(1)—Cl(1)	93.56(3)	Cl(2)—Fe(1)—Cl(2A)	81.625(12)
N(1)—Fe(1)—Cl(2)	97.92(3)	Cl(1)—Fe(1)—Cl(2)	98.539(14)
N(2)—Fe(1)—Cl(2)	89.29(3)		

4.4 ± 0.2 min, 6.6 ± 0.2 min, and 7.4 ± 0.2 min, respectively. Other aromatic compounds were analyzed by GC (7820A) and GC–MS (7890-5975C). The temperature of the GC column/GC–MS column was set at 60 °C for 1 min and then was programed to rise to 250 °C at the rate of 15 °C min^{-1}.

3. Results and discussion

3.1. Synthesis and characterization of complex $Fe_2\mathbf{L}_2(\mu_2\text{-}Cl)_2Cl_2$

Ligand **L** was prepared using modified literature procedure [31] and has reported in our previous work [25]. Treatment of ligand **L** and $FeCl_2 \cdot 4H_2O$ in methanolic solution for 3 h leads to the formation of dinuclear iron(II) complex $Fe_2\mathbf{L}_2(\mu_2\text{-}Cl)_2Cl_2$ in a yield of 76% (Scheme 1). The complex is easy to purify by successively washing with water and diethyl ether for several times. The identity of complex $Fe_2\mathbf{L}_2(\mu_2\text{-}Cl)_2Cl_2$ was confirmed by its microanalysis and X-ray crystal structure determination.

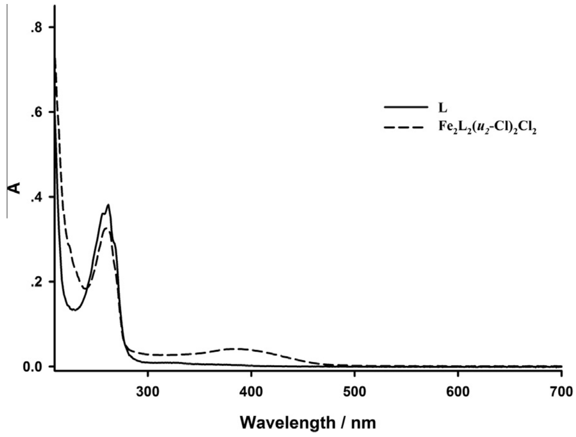

Fig. 2. UV–Vis spectra of ligand **L** and complex $Fe_2\mathbf{L}_2(\mu_2\text{-}Cl)_2Cl_2$ in MeCN.

Crystals of complex $Fe_2\mathbf{L}_2(\mu_2\text{-}Cl)_2Cl_2$ suitable for X-ray single crystal diffraction analysis were grown from a methanol solution into which the vapor of diethyl ether was diffused. Its structure is shown in Fig. 1 and its crystallographic data and selected bonding parameters are tabulated in Tables 1 and 2, respectively. The structure consists of a dimeric unit generated through a crystallographically imposed inversion center. Each iron center is bridged by two chloride ligands and bound terminally by a chloride and a ethyne-substituted bis(pyridin-2-ylmethyl)amine ligand to construct a pseudo-octahedral geometry with "N_3Cl_3" donor atoms. As expected, the $Fe—N_{amine}$ distance (2.3126(11) Å) is more than 0.1 Å longer than $Fe—N_{pyridine}$ (2.2083(11), 2.2156(11) Å), which is similar to reported analogous iron complexes [32–36]. The two Fe—Cl(bridging) bond distances (Fe(1)—Cl(2) = 2.4797(4) Å, Fe(1)—Cl(2A) = 2.5445(4) Å) are over 0.1 Å longer than the Fe—Cl (terminal) bond distances (Fe(1)—Cl(1) = 2.3667(4) Å), but both of them still falls within the range observed in structurally related complexes [32–37]. The Fe…Fe distance is 3.803(4) Å, which falls at the top end of the range found for related complexes [32–37].

The UV spectra of ligand **L** and complex $Fe_2\mathbf{L}_2(\mu_2\text{-}Cl)_2Cl_2$ were recorded in acetonitrile. It exhibits a very strong absorption in the UV, corresponding mainly to pyridines π–π^* transitions, and a less intense one near visible region related to metal-to-ligand charge transfer (MLCT) that are responsible for the yellow color of the solution (Fig. 2).

The cyclic voltammogram (CV) of complex $Fe_2\mathbf{L}_2(\mu_2\text{-}Cl)_2Cl_2$ showed a broad quasi-reversible redox couple and the oxidation event which assigned to Fe^{2+}/Fe^{3+} was at a low potential of −0.129 V ($E_{1/2}$) (versus Fc^+/Fc) as illustrated in Fig. 3. This broad redox couple can be explained by the structure of complex $Fe_2\mathbf{L}_2(\mu_2\text{-}Cl)_2Cl_2$ composing two iron(II) metal center. Although those two iron(II) metal center possess exactly the same coordination sphere as revealed by its solid state structure, the CVs of them may not exhibit the same redox events. This assumption was also supported by the differential pulse voltammograms shown in

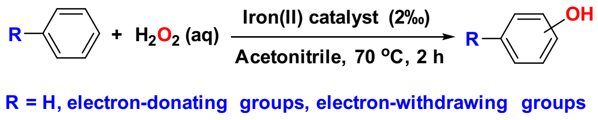

Scheme 2. Hydroxylation of aromatic compounds catalyzed by complex $Fe_2\mathbf{L}_2(\mu_2\text{-}Cl)_2Cl_2$.

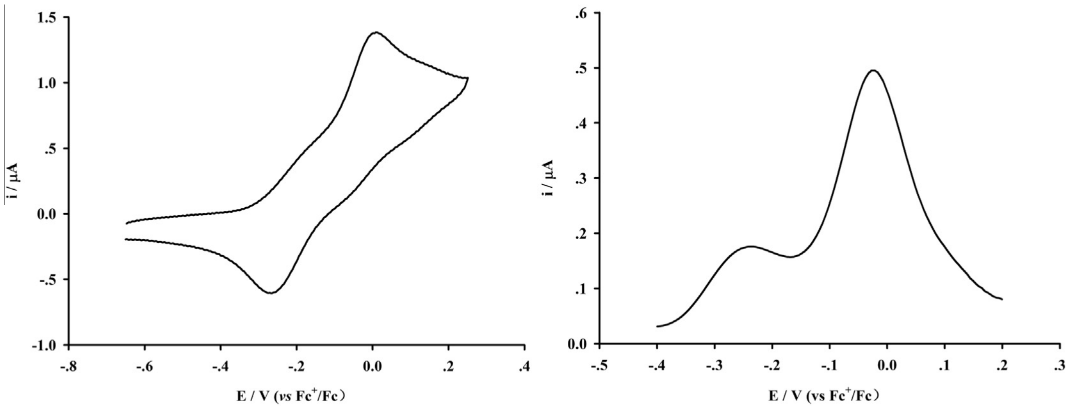

Fig. 3. Left: Cyclic voltammogram of complex $Fe_2\mathbf{L}_2(\mu_2\text{-}Cl)_2Cl_2$ in acetonitrile (v = 0.1 V s^{-1}, 298 K); right: differential pulse voltammogram of complex $Fe_2\mathbf{L}_2(\mu_2\text{-}Cl)_2Cl_2$ in acetonitrile (v = 0.1 V s^{-1}, 298 K).

Table 3
Products distribution and yields (area ratio %)[a] for the hydroxylation of aromatic compounds with H_2O_2.

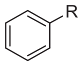	Conversion[b] (%)	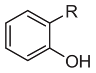	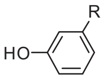	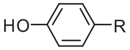	Other products				
R = H	24.8 ± 0.5	74 ± 4	–	–	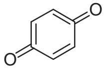 (1.0 ± 0.5)	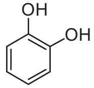 (5 ± 2)	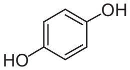 (20 ± 2)		
R = Cl	23.4 ± 0.2	35 ± 2	–	51 ± 4	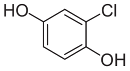 (10 ± 1)	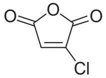 (4 ± 1)			
R = Br	21.1 ± 0.3	27 ± 2	47 ± 2	–	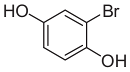 (21 ± 2)	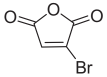 (5 ± 1)			
R = CN	20.0 ± 0.3	44 ± 3	24 ± 1	32 ± 1	–				
R = NO_2	19.8 ± 0.7	12 ± 1	61 ± 1	27 ± 1	–				
R = Me[c]	25.7 ± 0.2	21 ± 2	20 ± 2	–	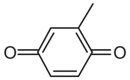 (8 ± 1)	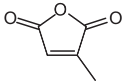 (3 ± 1)	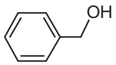 (15 ± 1)	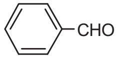 (25 ± 1)	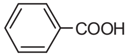 (8 ± 1)
R = OMe	27.8 ± 0.9	45 ± 1	–	24 ± 1	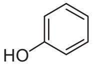 (22 ± 2)	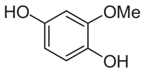 (9 ± 1)			
R = Ph	28.0 ± 0.4	25 ± 2	23 ± 1	25 ± 1	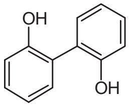 (1.0 ± 0.2)	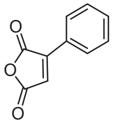 (6 ± 1)	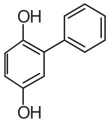 (17 ± 1)	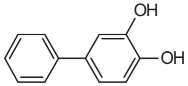 (3 ± 1)	
R = ^{t}Bu	18.0 ± 0.9	–	16 ± 1	49 ± 3	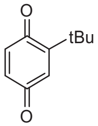 (14 ± 1)	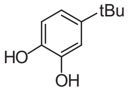 (17 ± 1)	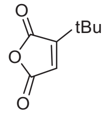 (4 ± 1)		

[a] Calculated by GC–MS.
[b] Calculated by single addition method with toluene as internal standard substance, GC.
[c] Benzene as internal standard substance.

Fig. 3, which displayed two successive oxidation peaks at −0.237 V and −0.024 V, respectively.

3.2. Catalytic hydroxylation of aromatic compounds

We began our evaluation of this iron-based catalyst by hydroxylation of benzene using hydrogen peroxide as an oxidant in acetonitrile and the hydroxylation was carried out under different conditions by varying reaction temperature, reaction time, catalyst dosage and the amount of H_2O_2. Full details of the optimization of the reaction conditions are reported in our recent work [25]. By employing the optimized reaction conditions, benzene conversion achieves 24.8% with a selectivity of 74% by using complex $Fe_2\mathbf{L}_2(\mu_2\text{-}Cl)_2Cl_2$ as a catalyst.

Inspired by higher selectivity than other catalytic systems we reported previously [25,26], we tried to extend the hydroxylation

Table 4
Variation in product distribution at various reaction time.[a]

Substrate	0.5 h	1 h	1.5 h	2.0 h
Benzene	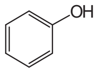 (10.3%)	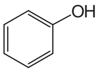 (12.0%) 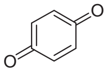 (0.8%)	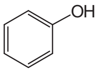 (15.3%) 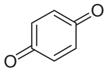 (1.4%)	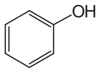 (19.8%) 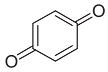 (2.1%) 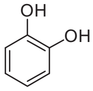 (0.6%) 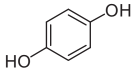 (0.7%)
Toluene	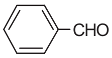 (11.6%) 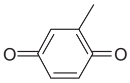 (2.9%) 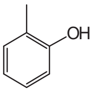 (11.9%) 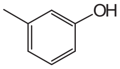 (2.2%)	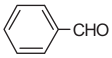 (13.1%) 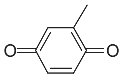 (2.3%) 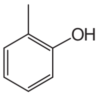 (10.5%) 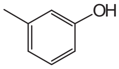 (2.4%)	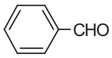 (12.9%) 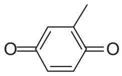 (3.6%) 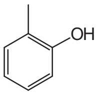 (13.0%) 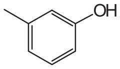 (4.1%) 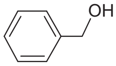 (0.9%)	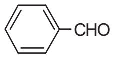 (14.6%) 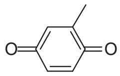 (3.9%) 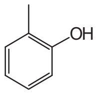 (13.3%) 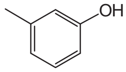 (5.0%) 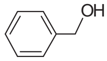 (1.3%) 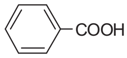 (2.9%)
Chlorobenzene	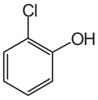 (13.9%) 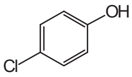 (2.6%)	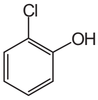 (14.6%) 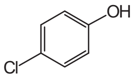 (4.0%)	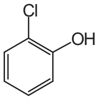 (15.1%) 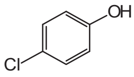 (4.7%)	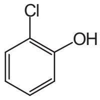 (15.3%) 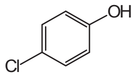 (4.7%) 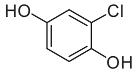 (2.0%) 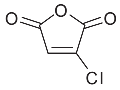 (0.8%)

---

[a] The yield of products (area ratio %) are calculated by GC–MS.

reaction to substituted aromatic compounds under the reaction conditions we optimized (Scheme 2) [25]. The hydroxylation of aromatic compounds with both electron-donating substituents and electron-withdrawing substituents afforded the corresponding phenols in moderate yield (10–20%) with the distribution of isomers of *ortho*-(*o*), *meta*-(*m*) and *para*-(*p*), although most of them produced other by-products with a certain percentage (Table 3). In general, aromatic compounds with electron-donating substituents (Me, OMe, Ph) could be hydroxylated in higher reaction conversion than those with electron-withdrawing substituents (NO_2, CN, Br, Cl). The only exception is *tert*-butylbenzene, which exhibited the lowest conversion probably due to the steric effect of the *tert*-butyl group. On the contrary, aromatic compounds with electron-withdrawing substituents (74–100%) showed higher hydroxylation selectivity than those with electron-donating substituents (41–73%), although the distribution of *o*-, *m*- and *p*-position phenols do not have distinct regularity. The *m*-hydroxylated products obtained higher than other isomers suggest that the hydroxylation occurred preferably at the *meta*-position for the aromatics with electron-withdrawing groups such as nitrobenzene and bromobenzene. But no formation of *m*-hydroxylated product was found when chlorobenzene used as the substrate and cyanobenzene favor to form *o*-hydroxylated product. The predominance of the *p*-substituted phenol and no *o*-substituted phenol formation in *tert*-butylbenzene oxidation indicate that the oxidizing species is sterically demanding, which is consistent with the reported analogous systems [38,39]. For the aromatic compounds with electron-donating substituents, some by-products such as di-hydroxylated derivatives, quinones and oxidative ring-opening adducts were detected. In the case of toluene, the oxidation took place at the methyl group, giving benzaldehyde, benzoic alcohol and benzoic acid in a yield of 6.4%, 3.9% and 2%, respectively. Interestingly, phenol was obtained in 6.1% yield in the case of anisole, which indicates demethylation happened in the oxidation process. It is noteworthy that for most of the substrates, a derivative of maleic anhydride was observed. This can certainly be attributed to the well established fact that the deep oxidation of benzene skeleton produced this anhydride. This argument was further validated by monitoring the reaction progress, Table 4. As shown in the table, along the reaction coordinate, the reaction products became complicated and for the chlorobenzene, the chloro-substituted maleic anhydride was observed in the products at the reaction time of 2 h.

3.3. Mechanistic considerations

In order to obtain some insights into the general type of mechanism involved in the studied oxidations, we selected benzene as an example to perform the reaction in the presence of a radical scavenger as well as some control experiments. The results are tabulated in Table 5.

Generally, in the oxidation of benzene by H_2O_2 using iron complex as catalyst, the hydroxyl radicals are considered as active species for the hydroxylation [40,41]. When a radical scavenger, such as ethanol and TEMPO (2,2,6,6-tetramethylpiperidine-1-oxyl), was added into the oxidation of benzene by complex $Fe_2\mathbf{L}_2(\mu_2\text{-Cl})_2Cl_2$, the phenol yield decreases steadily while the phenol selectivity increases slightly (Table 5, entries 4–8 and 11–13). These observations are in agreement with what we reported previously for Fe (III) and Cu (II) catalytic systems [25,26]. In the oxidation process, the added either ethanol or TEMPO scavenges most hydroxyl radicals to retard the benzene conversion and meanwhile to reduce over-oxidation of the phenol, which decreases the benzene conversion and improve slightly the reaction selectivity, respectively. The observations suggest that the oxidation of the aromatic compounds catalyzed by the diiron complex adopts analogously the same radical mechanism. However, as we pointed out previously [25], the participation of a high valent iron-oxo species cannot be ruled out since the oxidation occurred still even when excess radical scavenger was present.

Table 5
The influence of radical scavengers on the hydroxylation of benzene performances.

Entry	Radical scavenger	Conversion (%)	Yield (%)	Selectivity (%)
1[a]	–	24.8 ± 0.5	18.4 ± 0.6	74 ± 4
2[b]	–	0	0	0
3[c]	–	0	0	0
4	1 mmol EtOH	24 ± 1	18 ± 1	76 ± 2
5	6 mmol EtOH	18.7 ± 0.9	14.3 ± 0.7	77 ± 3
6	12 mmol EtOH	14.9 ± 0.5	11.6 ± 0.7	77.6 ± 0.9
7	24 mmol EtOH	11.3 ± 0.7	8.9 ± 0.3	79 ± 1
8	48 mmol EtOH	9.6 ± 0.7	8 ± 1	79 ± 1
9[b]	1 mmol TEMPO	0	0	0
10[d]	1 mmol TEMPO	0	0	0
11	6 mmol TEMPO	16.4 ± 0.9	12.7 ± 0.7	77 ± 2
12	12 mmol TEMPO	12 ± 1	9 ± 1	79 ± 2
13	24 mmol TEMPO	9.9 ± 0.4	8.0 ± 0.9	81 ± 2

[a] Reaction conditions: complex $Fe_2\mathbf{L}_2(\mu_2\text{-Cl})_2Cl_2$ (0.01 mmol), benzene (0.9 mL, 10 mmol), H_2O_2 (1.2 mL, 12 mmol), acetonitrile as solvent (3.8 mL), temp. = 70 °C, reaction time = 2 h.

[b] Under the standard conditions without H_2O_2.

[c] Under the standard conditions without complex $Fe_2\mathbf{L}_2(\mu_2\text{-Cl})_2Cl_2$.

[d] Under the standard conditions without complex $Fe_2\mathbf{L}_2(\mu_2\text{-Cl})_2Cl_2$ and irradiation for 2 h.

4. Conclusions

In summary, a dinuclear iron(II)-based catalyst was prepared and fully characterized. The complex was employed as a catalyst on the hydroxylation of substituted aromatics with H_2O_2 as an oxidant. Aromatic compounds with electron-donating substituents showed higher reaction conversion than those with electron-withdrawing substituents while the selectivity of hydroxylation was on the opposite. The results indicated that the hydroxylating products are not only influenced by the electronic effect, but also by the steric one.

Acknowledgements

The authors would like to thank the National Natural Science Foundation of China (Grant nos. 21301071, 21171073, 21371079), the Natural Science Foundation of Zhejiang Province (LQ13B010002) and the Government of Zhejiang Province (Qianjiang Professorship for X.L.) for supporting this work.

Appendix A. Supplementary material

CCDC 1429939 contains the supplementary crystallographic data for the complex. These data can be obtained free of charge from The Cambridge Crystallographic Data Centre via www.ccdc.cam.ac.uk/data_request/cif.

Supplementary data associated with this article can be found, in the online version, at http://dx.doi.org/10.1016/j.ica.2016.02.005.

References

[1] B.D. Sherry, A. Fürstner, Acc. Chem. Res. 41 (2008) 1500.

[2] S.F. Zhu, Q.L. Zhou, Nat. Sci. Rev. 1 (2014) 580.

[3] R. Bedford, P. Brenner, The Development of Iron Catalysts for Cross-Coupling Reactions, in: E. Bauer (Ed.), Iron Catalysis II, Springer International Publishing, 2015, p. 19.

[4] D.S. Mérel, M.L.T. Do, S. Gaillard, P. Dupau, J.L. Renaud, Coord. Chem. Rev. 288 (2015) 50.

[5] Z. Xue, D. He, X. Xie, Polym. Chem. 6 (2015) 1660.

[6] W. Nam, Acc. Chem. Res. 40 (2007) 465.

[7] E.G. Kovaleva, J.D. Lipscomb, Nat. Chem. Biol. 4 (2008) 186.
[8] E.I. Solomon, T.C. Brunold, M.I. Davis, J.N. Kemsley, S.K. Lee, N. Lehnert, F. Neese, A.J. Skulan, Y.S. Yang, J. Zhou, Chem. Rev. 100 (2000) 235.
[9] M. Costas, M.P. Mehn, M.P. Jensen, L. Que, Chem. Rev. 104 (2004) 939.
[10] X.M. Liu, S.K. Ibrahim, C. Tard, C.J. Pickett, Coord. Chem. Rev. 249 (2005) 1641.
[11] F. Gloaguen, T.B. Rauchfuss, Chem. Soc. Rev. 38 (2009) 100.
[12] C. Tard, C.J. Pickett, Chem. Rev. 109 (2009) 2245.
[13] T.R. Simmons, G. Berggren, M. Bacchi, M. Fontecave, V. Artero, Coord. Chem. Rev. 270–271 (2014) 127.
[14] S. Friedle, E. Reisner, S.J. Lippard, Chem. Soc. Rev. 39 (2010) 2768.
[15] B.J. Wallar, J.D. Lipscomb, Chem. Rev. 96 (1996) 2625.
[16] P.M. Vignais, B. Billoud, Chem. Rev. 107 (2007) 4206.
[17] D. Bianchi, R. Bortolo, R. Tassinari, M. Ricci, R. Vignola, Angew. Chem., Int. Ed. 39 (2000) 4321.
[18] E.V. Kudrik, A.B. Sorokin, Chem. Eur. J. 14 (2008) 7123.
[19] R.R. Fernandes, M.V. Kirillova, J.A.L. da Silva, J. da Silva, A.J.L. Pombeiro, Appl. Catal. A: Gen. 353 (2009) 107.
[20] X. Wang, T.Y. Zhang, B. Li, Q.S. Yang, S. Jiang, Appl. Organomet. Chem. 28 (2014) 666.
[21] A.E. Wendlandt, A.M. Suess, S.S. Stahl, Angew. Chem., Int. Ed. 50 (2011) 11062.
[22] A.M. Kirillov, M.V. Kirillova, A.J.L. Pombeiro, Coord. Chem. Rev. 256 (2012) 2741.
[23] A.M. Kirillov, M.V. Kirillova, A.J.L. Pombeiro, Homogeneous Multicopper Catalysts for Oxidation and Hydrocarboxylation of Alkanes, in: R. VanEldik, C.D. Hubbard (Eds.), Adv. Inorg. Chem., 2013, p. 1.
[24] A. Conde, M. Mar Diaz-Requejo, J. Perez, Chem. Commun. 47 (2011) 8154.
[25] B.B. Xu, W. Zhong, Z.H. Wei, H.L. Wang, J. Liu, L. Wu, Y.G. Feng, X.M. Liu, Dalton Trans. 43 (2014) 15337.
[26] L. Wu, W. Zhong, B.B. Xu, Z.H. Wei, X.M. Liu, Dalton Trans. 44 (2015) 8013.
[27] X.L. You, Z. Wei, B.B. Xu, X.M. Liu, Polyhedron 81 (2014) 743.
[28] X.H. Zeng, Z.M. Li, X.M. Liu, Electrochim. Acta 55 (2010) 2179.
[29] X.H. Zeng, Z.M. Li, Z.Y. Xiao, Y.W. Wang, X.M. Liu, Electrochem. Commun. 12 (2010) 342.
[30] G.M. Sheldrick, Acta Crystallogr., Sect. A 64 (2008) 112.
[31] D. Gonzalez Cabrera, B.D. Koivisto, D.A. Leigh, Chem. Commun. (2007) 4218.
[32] D.A. Handley, P.B. Hitchcock, T.H. Lee, G.J. Leigh, Inorg. Chim. Acta 314 (2001) 14.
[33] V.C. Gibson, R.K. O'Reilly, D.F. Wass, A.J.P. White, D.J. Williams, Dalton Trans. (2003) 2824.
[34] R. Cowdell, C.J. Davies, S.J. Hilton, J.D. Marechal, G.A. Solan, O. Thomas, J. Fawcett, Dalton Trans. (2004) 3231.
[35] C.J. Davies, G.A. Solan, J. Fawcett, Polyhedron 23 (2004) 3105.
[36] P.L. Pawlak, M. Panda, R. Loloee, B.E. Kucera, J.P. Costes, J.P. Tuchagues, F.A. Chavez, Dalton Trans. 40 (2011) 2926.
[37] M. Ito, Y. Takita, K. Sakai, T. Tubomura, Chem. Lett. 27 (1998) 1185.
[38] D. Bianchi, M. Bertoli, R. Tassinari, M. Ricci, R. Vignola, J. Mol. Catal. A: Chem. 200 (2003) 111.
[39] K. Kamata, T. Yamaura, N. Mizuno, Angew. Chem., Int. Ed. 51 (2012) 7275.
[40] D.H. Bremner, A.E. Burgess, F. Li, Appl. Catal., A 203 (2000) 111.
[41] G.B. Shul'pin, G.V. Nizova, Y.N. Kozlov, L.G. Cuervo, G. Süss-Fink, Adv. Synth. Catal. 346 (2004) 317.